Measurement of small strains in a noisy environment

M. S. Tillack,[a] M. S. Kazimi, and L. M. Lidsky

Department of Nuclear Engineering, Massachusetts Institute of Technology, Cambridge, Massachusetts 02139

(Received 11 December 1984; accepted for publication 3 June 1985)

A simple technique is demonstrated for measuring strains in an electromagnetically noisy environment using electrical strain gauges. For applications in which strains are produced electromagnetically in current-carrying structures, the noise signal can be much larger than the strain signal. Furthermore, the noise signal is at precisely the same frequency as the strain signal, making standard methods of synchronous signal detection difficult. This problem has been surmounted by modulating the detection circuit sensitivity. Bridge circuit modulation has been shown to effectively decouple the strain signal from the noise, even at very low strain levels of $\sim 10^{-8}$ m/m.

INTRODUCTION

The use of strain gauges is often desirable because of their low cost, high sensitivity, simplicity of use, and easy access in enclosed spaces. However, one major drawback is their susceptibility to electrical noise—unlike optical techniques of strain measurement. One particular application of strain measurement in an electromagnetic environment is in magnetic confinement fusion reactors, where the structural response of components to electromagnetic loads is an important issue. Plasma current transients induce currents in the surrounding conducting structures, which then interact with the large local magnetic fields to produce electromagnetic pressures, stresses, and strains. The magnitude of the induced stresses can be significant compared to the yield stresses of common structural materials, which may result in either abrupt failure or enhanced fatigue rates.

Most modern fusion reactor designs incorporate the effects of electromagnetic loads into the design of reactor components. Particular attention is given to major plasma disruptions, which have the most serious potential effects. Yet, the measurement of structural effects is not commonly performed in experiments operating today, which are predominantly designed to investigate plasma physics. This is in part due to the difficulty of measuring strains in the electromagnetic environment of a plasma experiment. The fact that the strains are caused by electric currents within the structural members implies that electrical strain gauges will be susceptible to large induced noise voltages that contain the same harmonic spectrum as the strain signals themselves. The large amount of synchronous noise would seem to make detection of the stresses difficult. To avoid the problems with electrical strain measurements, optical techniques have been suggested. However, optical techniques can present several undesirable features, including access requirements, complexity and, in some cases, limited sensitivity.

A technique is suggested here that could be applied to electrical strain measurements in structures that carry the electric currents responsible for the strains. By modulating the applied voltage on the Wheatstone bridge detection circuit, the strain signal can be separated from the noise signal using synchronous signal detection at the bridge frequency. In an ideal balanced bridge, the strain signal is the only signal that is affected by the bridge voltage. In the experiments described below, the induced currents are composed of a single frequency. This simplifies the measurement considerably because the detected strains are then also confined to a single frequency. In an actual fusion experiment, the detection must cover the full frequency spectrum inherent to a real plasma disruption or electromagnetic transient.

The detection technique and its application on a small benchtop experiment are described below. Electromagnetic strains in the experiment are induced by current-carrying filaments located at the center of a 64-mm-radius cylindrical copper shell. The small size of the experiment and, in particular, the small power supplies result in low strain levels of about 10^{-8} m/m and signal levels of about 1 μV. This difficulty was partly offset through the use of semiconductor strain gauges with gauge sensitivities over 100. Structural resonances are identified, and the measured strains are compared to "off-resonant" strains. Analytic and numerical predictions of the induced nonresonant strains confirm the validity of the measurements. Agreement at these low levels of strain is generally within 25%–50%.

I. EXPERIMENTAL APPARATUS

The test apparatus used to produce electromagnetic strains consists of four functional parts. As shown in Fig. 1, these are (1) the test piece and return current path, (2) the filaments and filament power supply, (3) the magnet and magnet power supply, and (4) the detection circuitry.

In the experiments, strains are produced by mechanisms analogous to those in a tokamak during disruption. Current-carrying "source" filaments simulate plasma currents, passing through the center of a cylindrical copper shell (see Fig. 2). The shell is 305 mm long, 64 mm in radius, and 0.38 mm thick, with a fairly large uncertainty in the thickness of 20%–30%, due to the difficulties in machining. The ends of the shell are connected with a low resistance return current path to allow the flow of axial current, which is the principal component induced. One of the ends of the shell (the bottom

 0034-6748/85/091706-06$01.30

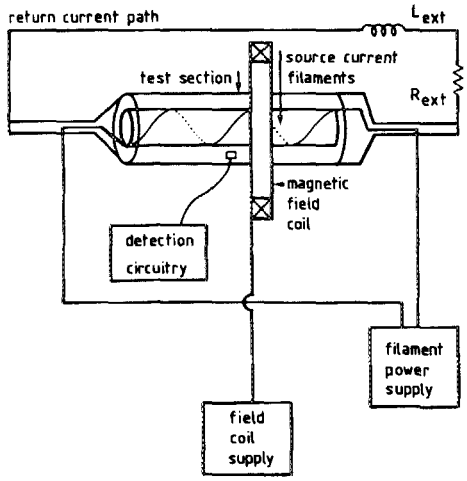

FIG. 1. Block diagram of the experiment.

end) is fixed, and the other end is left free, except for a small flange that allows for the connection to the return current shell.

The time-varying filament currents induce shell currents in the cylinder, which then undergo $J \times B$ forces with their own self-field, as well as with the filament fields. In addition, an external magnetic field coil is included to simulate interactions of the shell currents with the large toroidal magnetic field of a tokamak. In the tests, the structure is a continuous cylinder. The filaments are grouped into two sets, each spanning $\pi/2$ rad, and given a helical pitch such that the source current turns halfway around the cylinder as it covers the axial length. This particular geometry was chosen to better model the plasma during disruptions. Other geometries have been studied, including a shell with a hole; the results are presented elesewhere.[1]

The level of current passing through the shell is ~ 1 kA rms. Single-frequency currents are used to simplify the power supply design and to enhance the signal-to-noise ratio, making detection simpler. Insofar as any time dependence can be treated as a sum of Fourier components, no essential loss of information is inherent in this method. In practice, the limitations of the power supply restrict the frequency range of operation to a fairly narrow band between 100–1000 Hz.

To obtain this fairly substantial amount of current, a transistor amplifier power supply was built using 18 bipolar power transistors mounted on thick copper plates for cooling. The output of this amplifier is passed through an iron core transformer designed to match the power supply to the load. Both the amplifier and the filaments are water cooled, dissipating on the order of 2–3 kW each.

The external magnetic field coil is also water cooled and is capable of supplying 0.1 T on axis, with a 250-mm-diameter bore. As with the transistor amplifier, the dc power supply used for driving the current is a modified Airco "bumblebee" type arc welder.

The detection circuitry consists of rosettes of semiconductor strain gauges that are used as elements in a self-balancing ac Wheatstone bridge circuit. Two rosettes are placed at different axial locations on the cylinder: one at $L/2$ and one at $3L/4$. The rosettes are composed of three individual backed gauges (BLH Electronics, Model SPB3-06-12) oriented at 0°, 45°, and 90° from the horizontal. A minimum of three gauges is required to reconstruct the entire state of plane strain.

Self-balancing of the bridge circuit is accomplished by sensing the dc voltage across the bridge, amplifying the imbalance voltage by 10^6, and then using this signal to drive the gate of a low-resistance FET transistor that is placed in one of the legs of the bridge. Figure 3 shows a schematic diagram of the bridge circuit. Signal voltages are discouraged from

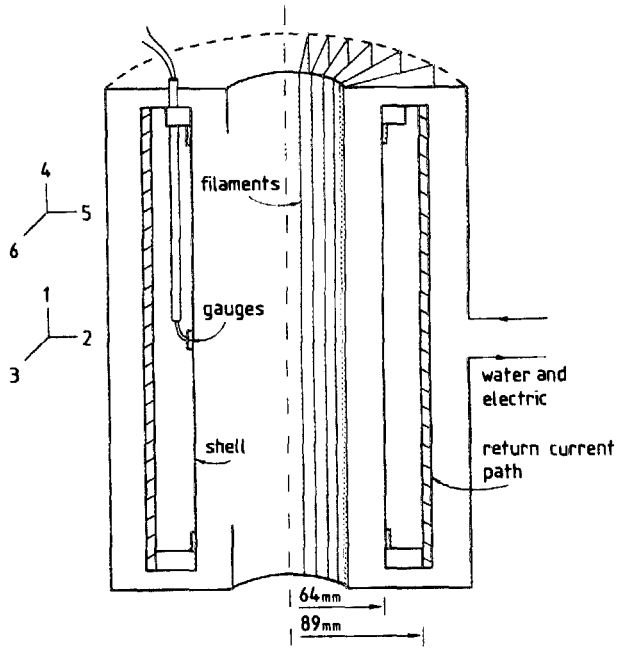

FIG. 2. Diagram of the test section. Gauge numbers, positions, and orientations are indicated at left.

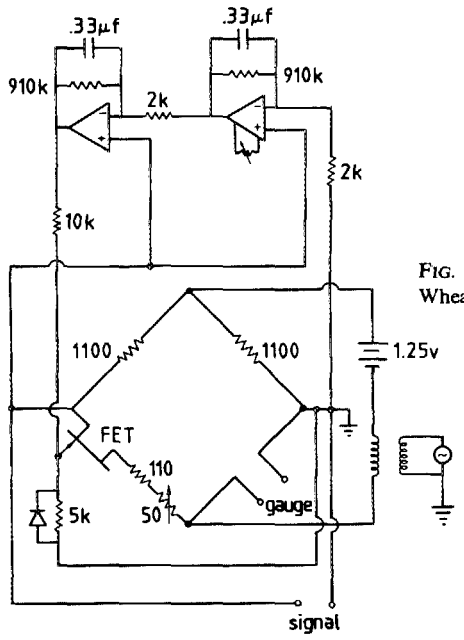

FIG. 3. Self-compensating Wheatstone bridge circuit.

being balanced by this circuit using high-pass filters on the 10^6 amplifier.

The output of the bridge circuit is passed through amplifiers and filters and is finally sent to a Keithley model 840 lock-in amplifier for processing. The lock-in amplifier measures only signals that occur at the frequency (or harmonic) of the signal supplied to the reference channel. This is accomplished internally by multiplying the input signal by the reference frequency and then time averaging. Figure 4 summarizes the entire array of electronics.

The reference channel of the lock-in amplifier is driven by electronic circuitry, which selects only the frequency at which the strains are expected to occur. For self-interactions and interactions of the shell current with the filament fields, the proper frequency is the sum of twice the filament current frequency plus the Wheatstone bridge frequency. For interactions with the external field, the correct frequency is the simple sum of the filament current frequency and the bridge frequency, because the external field is dc. These frequencies result from the fact that multiplying sinusoidal functions is equivalent to adding their frequencies. The signal voltage V_s (ignoring bridge circuit nonlinearities) is proportional to the bridge voltage V_b, and to the perturbed resistance of the gauge R

$$V_s(t) = k_1 V_b(t) R(t), \tag{1}$$

where k_1 is some constant depending on the circuit values. The time-varying part of the resistance is directly proportional to the strain, which is given by the product of the field and the shell current

$$R(t) = k_2 I(t) B(t), \tag{2}$$

where k_2 accounts for the gauge sensitivity and the conversion of the induced pressures into strains (all of which are linear processes). The time dependence of the current, bridge voltage, and magnetic field are given by

$$I(t) = I_0 \cos(\omega_1 t), \tag{3}$$

$$V_b(t) = V_{bo} \cos(\omega_2 t + \phi_2), \tag{4}$$

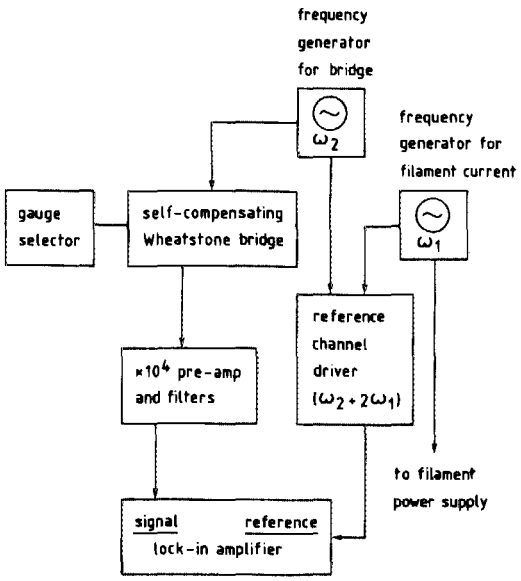

FIG. 4. Block diagram of the detection electronics.

$$B(t) = B_0 \cos(\omega_1 t + \phi_1),$$

or

$$B(t) = B_{\text{ext}}, \tag{5}$$

where I is the shell current and B is the field at the shell. The output voltage of the bridge is, therefore, given by

$$V_s = k_3 \cos(\omega_1 t)\cos(\omega_2 t + \phi_2)\cos(\omega_1 t + \phi_1)$$

or

$$V_s = k_3 \cos(\omega_1 t)\cos(\omega_2 t + \phi_2). \tag{6}$$

II. DESCRIPTION OF TESTS

A. Procedure

To accumulate the data, the shell is rotated with respect to the filaments to cover a full period of the source current. This minimizes the number of strain gauges needed for spatial measurements. At each shell position, a reading is taken for each gauge, including signal strength and phase angle. Using sinusoidal loading, each point of the structure undergoes both tension and compression during every cycle. The relative phase angle is therefore an important indicator to correctly distinguish at a given instant which points are in tension and which are in compression. As the shell angle is varied, the phase angle passes through 180° at node points separating tension and compression. As the frequency is varied, the phase angle shows strong variations at structural resonances.

Several simple tests can be performed to determine the amount of interference from noise, e.g., reproducibility checks and verification of the functional dependence of strain versus current. (For self-interactions, the strain should vary as I^2; for interactions of the induced current with a steady external field, the scaling is linear.) Another good test is to vary the bridge voltage to determine whether or not the signal strength is proportional to the bridge voltage. These tests help to determine the amount of interference from noise and the validity of the measurement.

B. Sources of error

The strain is a secondary quantity, in the sense that it results from the induced currents and fields that are, themselves, direct consequences of the source current transient. This fact makes it very difficult to trace sources of error in the measurements, insofar as there is no direct indication available of the induced current distribution. Direct measurement of these currents would be useful but very difficult.

Sources of error include machining tolerances, spatial measurement limitations, power supply characteristics, and detection electronics.

The largest machining tolerance is on the shell thickness. This does not affect the accuracy of the strain measurement but, rather, the accuracy of comparisons between predicted versus measured responses.

The finite size of the gauges limits the measurement resolution to ~1.5 mm in the direction of the gauge axis. In addition, bonding of the individual gauges to the shell resulted in placement errors of about 1–2 mm and errors in the rosettte angles of about 5°. This uncertainty is particularly important for measurements near the hole, where very steep

gradients occur. Furthermore, positioning of the gauges relative to the source current is uncertain by $\sim 5°$.

The waveform reaching the filaments through the series of amplifiers and transformers is far from purely sinusoidal. Waveform distortion at higher harmonics of the base frequency is particularly bothersome because it tends to pass through the detection electronics. This type of noise results from crossover distortion, transformer nonlinearity, and the current-dependent voltages in the power transistors. The result is error in the signal of 10% or more.

The final category of error sources includes all of the signal paths from the gauges to the lock-in amplifier. Noise signals are most crucial before the 10^3 preamp, which feeds the lock-in amplifier. These noise signals can be picked up through the air or through poor ground connections. The signal wires are coaxial wherever possible. Probably the worst source of noise comes from the gauges and gauge lead wires that either touch or run close to the surface containing currents greater than 1 kA. The minimum practical area for picking up signals at the gauges is ~ 1 mm^2. Using this area and the values of frequency and current present in the experiment, the level of synchronous noise coming from the exposed gauge area is $\sim 10\,\mu$V, or ~ 10 times the largest measured signals. Most of the signal levels are smaller than $1\,\mu$V, leading to synchronous signal-to-noise ratios in the range of 0.1–0.01.

The Wheatstone bridge circuit also contributes to detection circuit noise. The bridge circuit has simultaneously very large and very small signals contained within the same circuit. The greatest benefit from efforts to improve the signal quality would probably come from careful redesign and optimization of this circuit.

The total error in the measurements and comparison with predictions is of the order of 25–50%. This is admittedly rather high. In practical applications, many of these sources of error would be irrelevant, insofar as comparing with predictions is not the dominant concern. Also, in practical applications the signal levels would be much larger, such that relative detection errors could be expected to be much lower. (Noise tends to scale as I, whereas signal scales as I^2 or IB_{ext}.)

III. RESULTS

One of the consequences of using a thin shell for the test piece is the existence of widespread resonant behavior. After observing a high degree of frequency dependence in the strain signal, a careful frequency scan was made and the resulting gauge circuit response is presented in Fig. 5. Following this, an analysis of the modal vibrations of a cylinder was performed with an approximate analytic solution[2] and with the aid of a finite element structural code—PAFEC.

The results presented in Fig. 6 indicate two things: First, the resonances in Fig. 5 are probably due to $m/n = 2/1$ and 4/1 (where m and n are the circumferential and axial mode numbers, respectively), insofar as the source current spatial variation was periodic every π rad. Second, due in part to stimulation of higher harmonics, it is difficult to locate any region of frequency space that was not affected to some extent by resonant behavior. This further complicates the comparison of the data with numerical predictions.

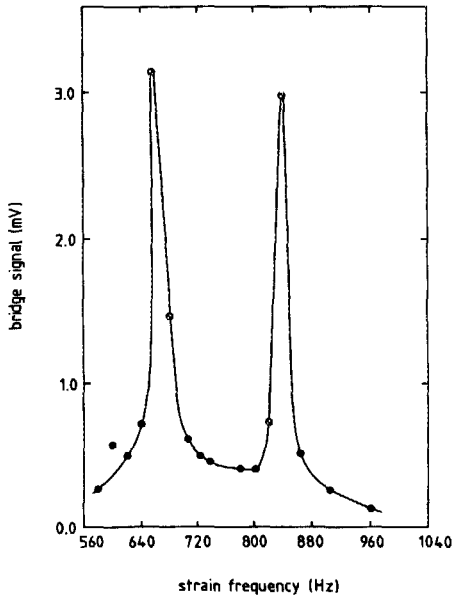

FIG. 5. Gauge response to strain resonances.

Figures 7 and 8 show the rms values of strain for self-field and external field interaction spanning π rad, or one full period of the source current. The peak level of strain for self-interactions is $\sim 1\times 10^{-8}$ and for external field interactions, $\sim 3\times 10^{-8}$. For these measurements, the gauge circuit sensitivity is $\sim 50\,\mu\text{V}/\mu\epsilon$, where the circuit sensitivity S_c, is given by

$$S_c = S_g(r/1 + r)V_g, \tag{7}$$

where S_g is the gauge sensitivity (120), r is the bridge-resistance ratio (10), and V_g is the voltage across the gauge (4.7 V).

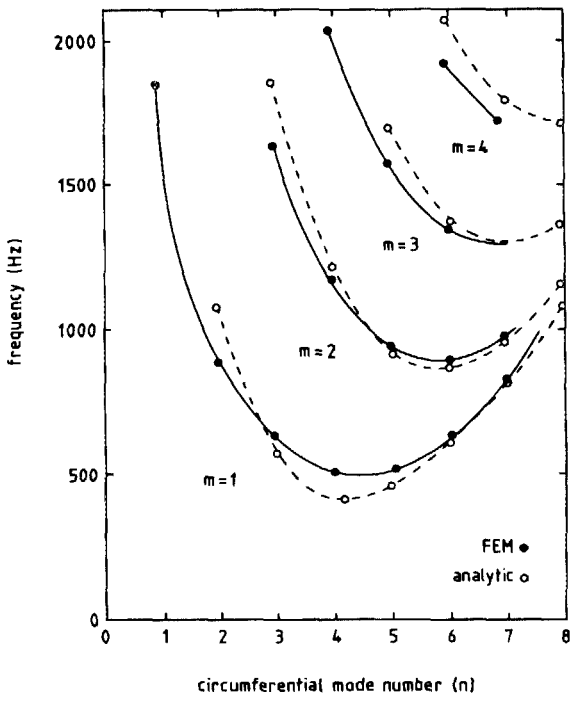

FIG. 6. Predicted modal resonances of the cylinder.

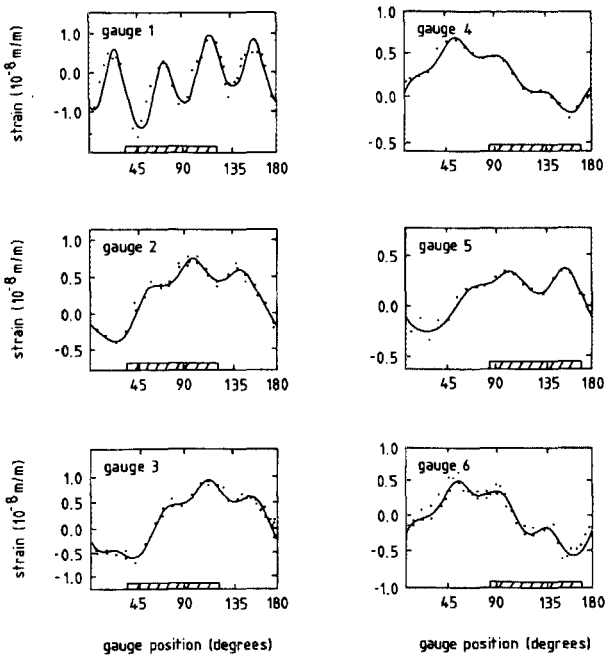

FIG. 7. Self-interactions data: rms time-averaged strain vs position on the shell. Position of the filament current is indicated by the hatched area.

Strains due to self-field and external field interactions are easily separated because they occur at different frequencies, and the detection circuitry provides measurements at individual frequencies. The most noticeable feature of the self-field data is the strong spatial harmonics—especially the first harmonic, which represents the interaction of the spatially constant Fourier component of the source current with the cos (2θ) component of the induced current, and vice versa. This is *not* a structural resonance, because care was taken to search frequency space for a nonresonant frequency. Rather, it is due to the spatial dependence of the induced currents and fields. Successively higher harmonics are more strongly damped. The external field interaction appears to contain, almost exclusively, the lowest Fourier component.

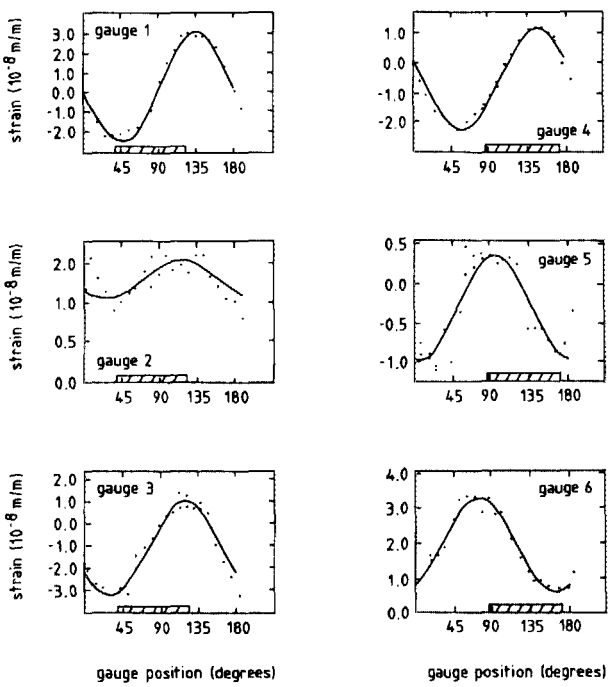

FIG. 8. External field interactions data: rms time-averaged strain vs position on the shell. Position of the filament current is indicated by the hatched area.

The measured stresses can be compared with simple order-of-magnitude estimates by assuming a central axial current transient in a uniform, unsupported shell. This is a crude estimate but should verify that the measurements provide values of strain that are in the correct range. In the experiments, the total axial-induced current is measured with a Rogowski coil, and the source current with a resistive shunt.

For the case of self-interactions, the forces are principally radial and result from the interaction of axial shell currents and the circumferential field due to the filament currents

$$p = \mathbf{K} \times \mathbf{B}, \tag{8}$$

where

$$K = I_s/2\pi r\ , \tag{9}$$

and

$$B = \mu_0 I_f/2\pi r. \tag{10}$$

The stress and strain are given simply by

$$\sigma = pr/t\ , \tag{11}$$

and

$$\epsilon = \sigma/E, \tag{12}$$

where σ is the circumferential stress, and E is the modulus of elasticity (11.7×10^{10} for copper). With $I_s = 750$ and $I_f = 1040$ A rms, the stress and strain obtained are $\sigma \approx 1000$ Pa and $\epsilon \approx 9\times10^{-9}$. This can be compared with Fig. 7, which shows a peak strain of $\sim 10^{-8}$.

For external field interactions, the forces are principally torsional. The force per unit axial length is given by

$$F' = IB_r. \tag{13}$$

The radial field in the experiment reaches a peak value of 80 G at the top, -80 G at the bottom, and varies roughly linearly in between. The peak torque and shear stress occur at the center of the shell ($x = L/2$) and are computed by integrating the force along the axial direction:

$$T = \int F' x\, dx = IB_{\max} L/12. \tag{14}$$

The shear stress in a thin-walled hollow cylinder is given by

$$\tau = T/2t\pi r^2. \tag{15}$$

Evaluating these equations results in a torque of 0.0465 Pa, a shear stress of 4750 Pa, and a normal strain (not shear strain) of roughly 4×10^{-8}. This can be compared with Fig. 8, which shows a peak strain of $\sim 3\times10^{-8}$.

More sophisticated numerical calculations were performed with a 2-D shell eddy current code and the PAFEC finite element structural code.[3] The eddy current code reduces the continuous structure into an equivalent matrix of discrete circuit elements and then solves a matrix circuit equation. In PAFEC, simple four-noded flat shell elements were used. The results at $L/2$ (150 mm) are presented and

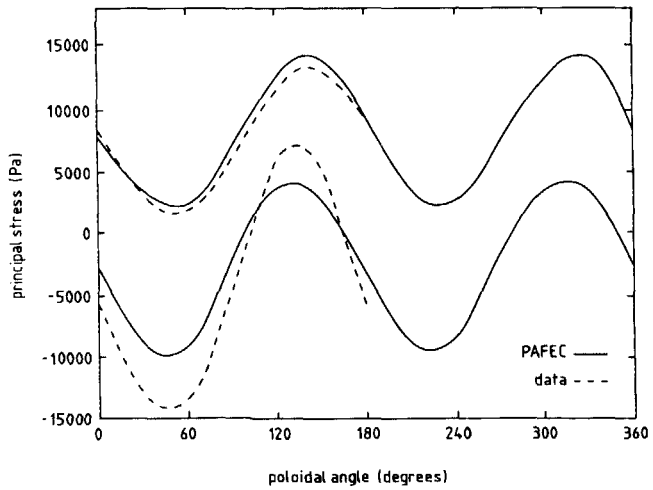

FIG. 9. Comparison of data and finite element code predictions for the external field interactions data.

compared with data for the external field interactions in Fig. 9. The principal stresses used for the comparison are obtained from the gauge data using standard plane stress transformations.[4] Agreement is well within the errors enumerated above.

IV. DISCUSSION

Small strains as low as 10^{-8} have been measured in a structure loaded electromagnetically. This demonstrates the possibility of using electrical strain gauges, even in applications where the synchronous electrical noise level is larger than the strain signal. This was accomplished by sinusoidally modulating the voltage on the detection circuit to separate the signal from the noise. In many applications with electromagnetic loading, the level of electric current will be much higher. This provides favorable scaling for detection, since noise tends to scale linearly with current, whereas parts of the strain signal scale as I^2.

In these experiments, the strain was excited at a single frequency. The full verification of this technique in applications with nonsinusoidal strains requires further study, because the detection technique would be somewhat different. For applications with a continuous spectrum of frequencies, including nonperiodic loading, the bridge voltage must be modulated at a frequency significantly higher than any strain frequency of interest. Then, high-pass filtering can be used to eliminate the noise signal. The viability of this technique at high frequency needs to be established.

ACKNOWLEDGMENT

This work was supported by the U.S. Department of Energy under Contract No. DE-AP07-79ID00019.

*Current address: Mechanical, Aerospace, and Nuclear Engineering Department, University of California, Los Angeles, California 90024.

[1]M. S. Tillack, M. S. Kazimi, and L. M. Lidsky, Department of Nuclear Engineering and Plasma Fusion Center, M.I.T., Report No. PFC/RR-83-30, October 1983.
[2]R. N. Arnold and G. B. Warburton, Proc. R. Soc. London **197**, 238 (1949).
[3]PAFEC 75 Theory Manual (PAFEC Ltd., Nottingham, England, 1976).
[4]C. C. Perry and H. R. Lissner, *The Strain Gage Primer* (McGraw–Hill, New York, 1962).